Pergamon

PII: S0038–092X(01)00076–7

Solar Energy Vol. 71, No. 6, pp. 403–414, 2001

0038-092X/01/$ - see front matter

www.elsevier.com/locate/solener

PERFORMANCE CHARACTERISTICS OF INTEGRAL TYPE SOLAR-ASSISTED HEAT PUMP

B. J. HUANG† and J. P. CHYNG
Department of Mechanical Engineering, National Taiwan University, Taipei, Taiwan

Received 27 September 1999; revised version accepted 31 May 2001

Communicated by DOUG HITTLE

Abstract—The characteristic of an integral type solar-assisted heat pump water heater (ISAHP) is investigated in the present study. The ISAHP consists of a Rankine refrigeration cycle and a thermosyphon loop that are integrated together to form a package heater. Both solar and ambient air energies are absorbed at the collector/evaporator and pumped to the storage tank via a Rankine refrigeration cycle and a thermosyphon heat exchanger. The condenser releases condensing heat of the refrigerant to the water side of the thermosyphon heat exchanger for producing a natural-circulation flow in the thermosyphon loop. A 105-liter ISAHP using a bare collector and a small R134a reciprocating-type compressor with rated input power 250 W was built and tested in the present study. The ISAHP was designed to operate at an evaporating temperature lower than the ambient temperature and a matched condition (near saturated vapor compression cycle and compressor exhaust temperature $< 100°C$). A performance model is derived and found to be able to fit the experimental data very well for the ISAHP. The COP for the ISAHP built in the present study lies in the range 2.5–3.7 at water temperature between 61 and 25°C.

1. INTRODUCTION

The direct expansion solar-assisted heat pump water heater (SAHP) has been studied by many researchers (for example, Sporn and Ambrose, 1955; Chaturvedi and Shen, 1984; O'Dell *et al*., 1984; Hino, 1995; Chaturvedi *et al*., 1998; Ito *et al*., 1999). A SAHP is composed of a Rankine refrigeration cycle coupled with a solar collector that acts as an evaporator. The refrigerant is directly expanded inside the evaporator to absorb the solar energy.

Depending upon the design and operating condition of a SAHP, heat may be dissipated to the ambient from the collector surface if the ambient temperature is lower than the collector temperature. But by a proper design of the Rankine refrigeration cycle and the collector for a specific operating condition, heat may be absorbed from, rather rejected to, the ambient. Under this condition, the refrigerant is directly expanded inside the evaporator to absorb energy from both solar radiation and ambient air.

It has been proven theoretically and experimentally that a high coefficient of performance (COP) of a SAHP can be obtained. The performance of a SAHP varies with solar radiation intensity and ambient conditions (wind speed and direction, temperature, humidity, etc.). A SAHP operates at a much more severe condition than a conventional air conditioner, usually at an unsteady state. Fig. 1 illustrates a possible time variation of the thermodynamic cycle for a SAHP. The design of a SAHP is thus quite complicated.

Chaturvedi *et al*. (1980) carried out a theoretical analysis for the instantaneous operation of a SAHP and shows that the evaporating temperature of a SAHP, T_e, depends on the solar radiation I and the ambient temperature T_a. T_e may be higher than T_a (heat dissipated to the ambient air from the collector) or lower than T_a (heat gained from the ambient air), depending upon the design and the operating conditions.

Chaturvedi *et al*. (1998) further shows theoretically and experimentally that a SAHP using a bare collector and a variable-frequency compressor has an optimum performance provided the collector temperature (related to the evaporating temperature T_e) is maintained in a temperature range of 5–10°C above ambient. Ito *et al*. (1999) also designed a SAHP with a bare collector operating at $T_e > T_a$.

It is worth noting that Chaturvedi *et al*. (1980) addressed the problem of system matching for the design of a SAHP. Whether a SAHP will operate at $T_e > T_a$ depends on the system matching and

†Author to whom correspondence should be addressed. Tel.: +88-62-2363-4790; fax: +88-62-2364-0549; e-mail: bjhuang@seed.net.tw

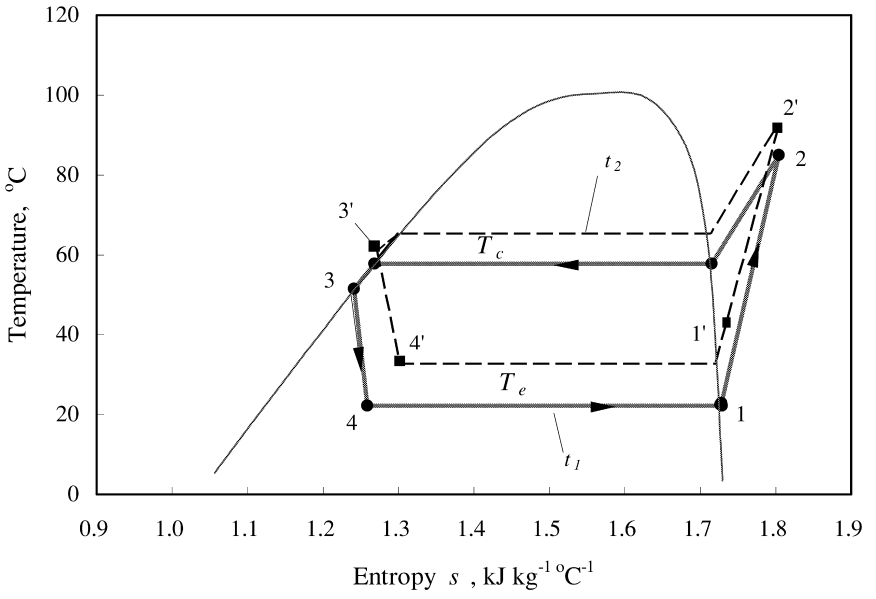

Fig. 1. Possible time variation of refrigeration cycle for an SAHP.

the weather condition. From engineering point of view, the consideration of system matching for the design of a SAHP should include efficiency and reliability. For a SAHP, the reliability problem results mainly from the operating temperature of the compressor. A high evaporating temperature T_e will cause a high compressor discharge temperature possibly exceeding the allowable temperature limit. Hence, a SAHP operating at $T_e < T_a$ has an advantage of having lower compressor exhaust temperature and dual heat source from both solar radiation and ambient air.

In the present study, we carried out outdoor experiment for an integral type solar assisted heat pump (ISAHP) (Huang and Chyng, 1999) and studied experimentally the characteristics of an ISAHP. We focus on the design of an ISAHP operating at $T_e < T_a$.

2. DESIGN OF AN INTEGRAL TYPE SOLAR-ASSISTED HEAT PUMP

As shown in Fig. 2, an integral type solar-assisted heat pump water heater (ISAHP) differs from the conventional design (Ito *et al*., 1999; Chaturvedi and Shen, 1984; Chaturvedi *et al*., 1998; O'Dell *et al*., 1984; Hino, 1995). The ISAHP consists of a Rankine refrigeration cycle and a water thermosyphon loop. The storage tank and the Rankine cycle unit of an ISAHP are integrated together to make a package heater. For avoiding using a water circulation pump and

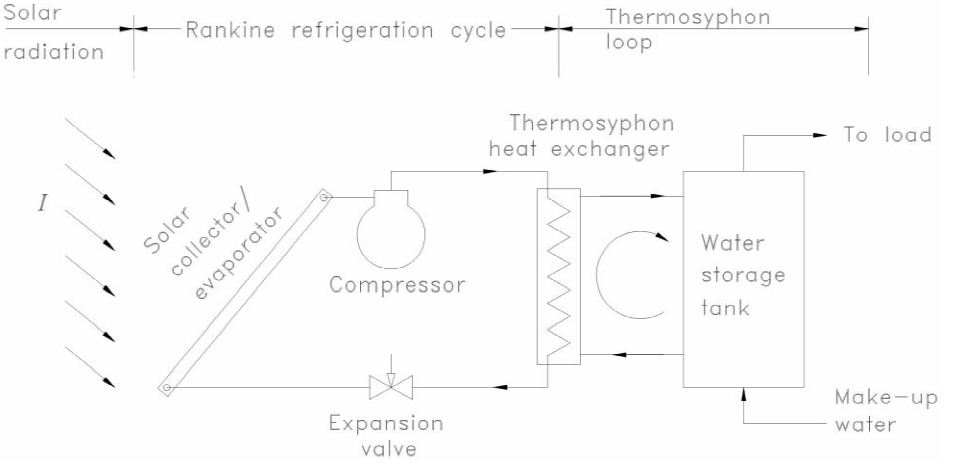

Fig. 2. Schematic diagram of ISAHP.

improving the system reliability, a thermosyphon loop is used to transfer the heat from the condenser to the water tank by natural circulation. A thermosyphon heat exchanger/condenser combines the condenser of the Rankine cycle and the heater of a thermosyphon loop together. A solar collector/evaporator unit combines the evaporator of the Rankine cycle and the solar collector.

The present ISAHP will absorb energy from solar radiation and ambient air simultaneously and then pumps the heat to the storage tank through a Rankine refrigeration cycle. The condenser releases condensing heat from the Rankine cycle to the water side of the heat exchanger for producing a natural-circulation flow in the thermosyphon loop. The water temperature T_w in the tank will vary with solar radiation, ambient conditions, load, and operational adjustment.

The instantaneous COP of an ISAHP may be a function of water temperature T_w, solar radiation intensity I, evaporating temperature T_e, and ambient conditions (temperature, humidity, and wind speed and direction, etc.). The system matching of the Rankine refrigeration cycle with the solar collector and the thermosyphon loop also plays an important role in the COP. The system matching includes the sizing of all the components of an ISAHP and the adjustment of the Rankine refrigeration cycle during operation. Chaturvedi *et al.* (1998) used a variable-frequency compressor for the adjustment during operation. The present study focuses on the adjustment of the expansion valve opening during operation for a better system performance.

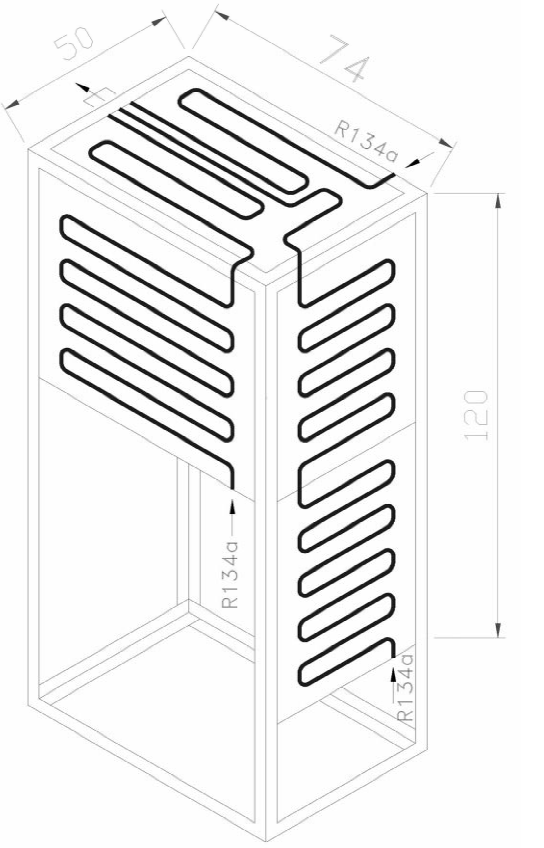

Fig. 3. Collector surface design of an ISAHP.

3. EXPERIMENTAL SETUP

3.1. Prototype design

An ISAHP was designed and fabricated in the present study. A bare collector/evaporator was adopted. The collector is of tube-in-sheet type using copper tube (6 mm diameter) and copper sheet (0.4 mm thick). Copper tubes are soldered on the copper sheet. The collector surface is divided into 4 parts: one top surface (50 cm × 74 cm), one front surface (50 cm × 120 cm) and two side surfaces (60 cm × 74 cm each), as shown in Fig. 3. The total surface area of the collector is 1.44 m^2. The collector surface is painted in black. Three refrigerant flow channels are made along the directions of front-to-top and side-to-top, all connected in parallel (Fig. 3).

The Rankine refrigeration cycle unit is mounted inside the ISAHP. A small R134a reciprocating-type hermetic compressor with piston swept volume 5.29 cc and rated input power 250 W is adopted. The motor speed of the compressor is 3520±10 rpm. The maximum allowable compressor discharge temperature is 120°C that is recommended by the manufacturer. The maximum current is 4 amperes. The compressor has a self-protection circuit to prevent from coil overheating and overcurrent. The volumetric efficiency of the compressor was provided by the manufacturer as

$$\eta_v = -0.0163 \times (P_2/P_1) + 0.6563 \quad (1)$$

The design of the thermosyphon heat exchanger in the thermosyphon loop is shown in Fig. 4. A helical-type coil made of copper tube with 6 mm diameter is immersed inside a straight water pipe. Water absorbs heat from the condensation effect of refrigerant vapor inside the copper tube and induces a bouyancy force for the natural circulation along the loop. The present ISAHP uses a 105-liter tank for hot water storage. The schematic diagram of the ISAHP is shown in Fig. 5.

An expansion valve (Model AEL-1, Egelhof, Germany) is used for the manual regulation of the refrigerant flow in the Rankine refrigeration cycle.

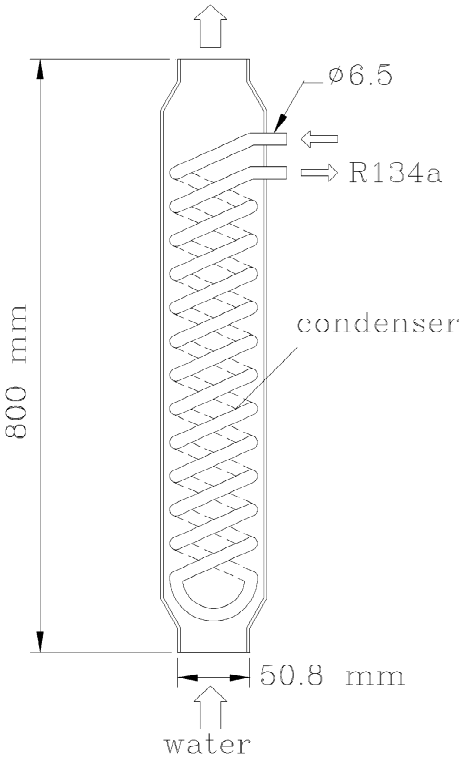

Fig. 4. Design of thermosyphon heat exchanger.

A receiver and a filter are installed downstream the condenser and an accumulator is installed downstream the collector/evaporator for protecting the compressor from wet compression.

3.2. Instrumentation

Two T-type thermocouples are installed in the suction and the discharge ports of the compressor for the temperature measurement, labeled as T_1 and T_2, respectively. Another two T-type thermocouples are installed at the upstream and the downstream of the expansion valve for the temperature measurement, labeled as T_3 and T_4, respectively, see Fig. 5. The uncertainty in temperature measurement is ± 0.8°C. Two pressure transducers (with an uncertainty of ± 0.02 bar) are used to measure the suction and the discharge pressures of the compressor, P_1 and P_2. The condensing temperature T_c is converted from the discharge pressure data P_1 using thermodynamic chart of R134a (ASHRAE, 1993). Since the pressure loss in the compressor suction line is rather large, the evaporating temperature T_e is determined from T_4, i.e. $T_e = T_4$. The solar radiation intensity I was measured by a pyranometer installed on a horizontal surface.

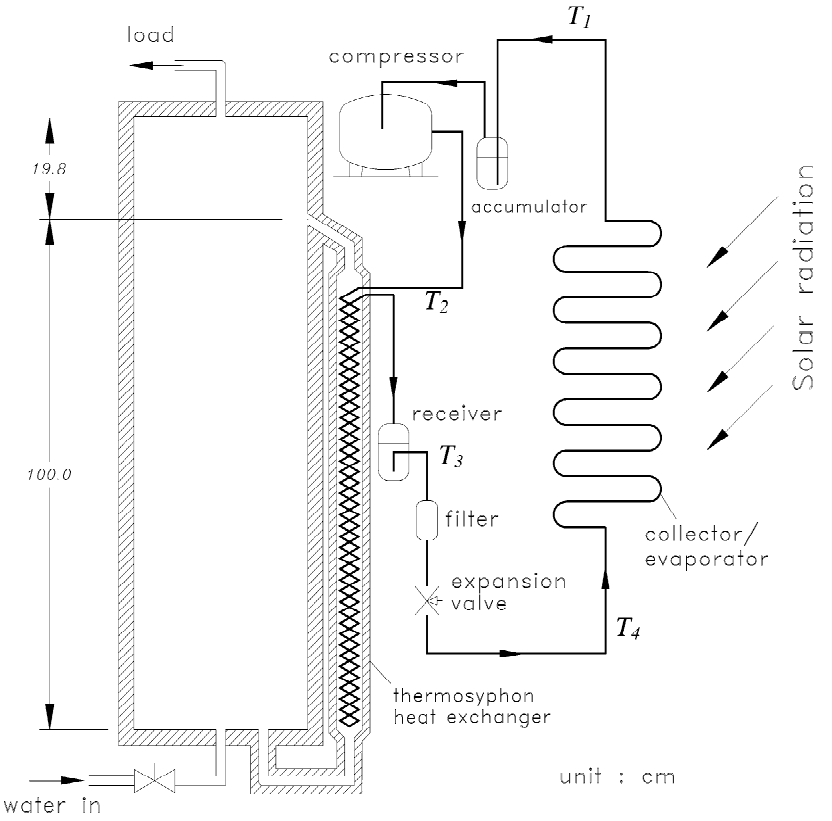

Fig. 5. Schematic diagram of integral-type solar assisted heat pump.

The instantaneous power input to the compressor W_{in} was measured by a power meter. The rate of energy rejected by R134a in the thermosyphon/heat exchanger (condenser) due to vapor condensation Q_c was determined by the relation:

$$Q_c = m_R(h_2 - h_3). \quad (2)$$

Q_c calculated from Eq. (2) will approximately equal to the rate of energy released to the water in the tank if the variation of temperature for various parts inside the condenser, including fluid and solid phases, is slow. Since the water in the tank, the condenser, and the evaporator/collector contain thermal mass, the temperature variation in these components is slow and can be considered at a quasi-steady state if the solar radiation varies not very fast. That is, the temperature variation at different parts of the ISAHP, including water and R134a, is induced mainly by solar radiation variation. In order to reduce the error caused by unsteady-state operation, the measured data need screening according to the steadiness of solar incident radiation *I*. Some experimental observations show that the thermal response time of the present ISAHP for an abrupt change of solar radiation is about 5 min. Hence, all the data are taken at the condition that the solar radiation intensity keeps steady for 5 min. The above quasi-steady condition and data screening applies to the test results presented in the present paper. The 95% confidence uncertainty range for all the test results is calculated and presented in the paper according to Kline and McClintock (1953).

4. TEST RESULTS

The ISAHP was tested outdoors under various conditions. Fig. 1 illustrates a possible time variation of the thermodynamic cycle. A preliminary test for a fixed expansion valve opening showed that the compressor exhaust temperature at high water temperature and high solar radiation would exceed the maximum tolerance 120°C.

In order to keep the compressor at a suitable operating condition, the expansion valve is adjusted manually during operation to keep the thermodynamic state at the suction port of the compressor close to a saturated vapor state (within±2°C) and the exhaust temperature is lower than 100°C. This is denoted as a *matched condition*. In addition, refrigerant R134a is charged into the ISAHP with a proper quantity to assure the above matched condition. The experimental data listed in Tables 1 and 2 are taken at matched condition.

4.1. Characteristic correlations of ISAHP

To derive a correlation for the performance of an ISAHP, we calculate the total energy absorbed at the evaporator Q_e according to Eq. (3):

$$Q_e = m_R(h_1 - h_4) \quad (3)$$

where m_R is the mass flowrate of the refrigerant; h_1 and h_4 are the enthalpy at the inlet and the outlet of the evaporator, respectively. h_1 and h_4 ($= h_3$ for isenthalpic process) are determined from the thermodynamic chart using the measured temperature and pressure. The results are shown in Tables 1 and 2. The uncertainty of Q_e is estimated to be ±10%. The refrigerant mass flow m_R is estimated from the compressor volumetric efficiency equation:

$$m_R = \eta_v \times V_{SW}/v_1 \quad (4)$$

where η_v is calculated from Eq. (1); v_1 is the specific volume of refrigerant at the suction port of the compressor; V_{SW} is the rate of compressor swept volume.

The expansion valve of the present ISAHP is adjusted during operation such that the evaporating temperature T_e is lower than the ambient temperature T_a and the ISAHP operates at *match condition*. Therefore, the total rate of energy absorbed in the evaporator Q_e consists of energy gained from solar radiation $Q_{solar}$and from the ambient heat Q_{air} and can be represented by the following relation:

$$Q_e = Q_{solar} + Q_{air} \quad (5)$$

The energy gained from the ambient air can be assumed to be proportional to the temperature difference between the evaporating and ambient temperatures and expressed as

$$Q_{air} = U_o A_c(T_a - T_e) \quad (6)$$

where U_o is the overall convective heat transfer coefficient from ambient air to solar collector surface.

The solar energy collected by the bare collector surface Q_{solar} can be assumed to be proportional to solar radiation intensity I:

$$Q_{solar} = \phi\alpha A_c I = A_{eff} I \quad (7)$$

where A_c is the total collector surface area; α is the effective absorption coefficient of the collector; ϕ is a geometric correction factor accounting for the sun angle to the ISAHP; A_{eff} ($= \phi\alpha A_c$) is the effective area for solar energy absorption.

Combining Eqs. (6), (7) with (5), we obtain

Table 1. Experimental data taken at matched operating condition (1)

No.	Date	Time	Solar radiation I (W/m^2)	Tank T_w (°C)	Ambient T_a (°C)	P_c kg/cm^2 (gage)	P_e kg/cm^2 (gage)	Thermodynamic states				Compressor W_{in} W
								T_1 (°C)	T_2 (°C)	T_3 (°C)	T_4 (°C)	
1	09/11/98	12:34	937	41.0	36.7	14.40	6.00	27.3	76.9	49.1	27.7	353
2	09/14/98	11:07	921	36.5	36.5	12.80	5.30	24.6	73.6	46.0	25.1	343
3	09/02/99	12:30	914	45.5	34.6	15.00	6.00	29.3	80.7	50.7	27.4	384
4	09/17/98	10:37	880	24.9	27.0	11.10	5.20	22.9	68.6	40.4	22.0	319
5	09/01/99	11:03	782	46.8	34.8	15.60	5.60	26.0	82.9	53.5	25.6	384
6	08/10/99	10:55	759	46.8	36.8	16.20	6.00	27.9	89.3	55.7	27.7	413
7	09/01/99	10:13	716	40.1	32.9	13.10	5.20	23.3	77.3	48.5	23.0	342
8	09/01/99	13:30	683	39.1	32.1	12.70	5.15	23.4	75.6	45.8	22.1	339
9	09/14/98	14:22	671	25.6	34.1	11.80	5.30	22.6	68.2	42.9	23.6	325
10	09/01/99	9:17	606	31.8	31.1	11.20	4.85	21.0	57.8	44.0	21.5	318
11	09/02/99	14:31	507	30.6	34.2	11.80	5.40	24.8	75.4	43.7	24.3	336
12	09/02/99	14:14	548	59.1	35.4	19.10	6.60	30.9	93.9	61.1	30.6	437
13	07/30/99	11:02	419	28.4	32.0	11.00	4.90	22.4	65.1	41.0	21.6	313
14	07/30/99	11:13	407	30.2	32.6	11.40	5.00	22.9	70.1	41.9	21.5	319
15	07/28/99	11:40	321	38.3	33.0	12.20	4.70	21.4	75.4	45.4	20.7	335
16	09/01/99	12:04	308	54.4	34.6	18.00	5.80	26.9	81.9	59.7	26.6	403
17	09/02/99	13:36	297	54.4	35.5	18.30	6.70	30.3	88.1	58.5	30.6	436
18	09/01/99	12:25	246	29.2	33.6	11.70	4.95	21.9	75.0	44.1	21.9	327
19	07/30/99	14:55	242	60.8	36.1	19.80	5.40	25.1	96.6	63.2	25.1	429
20	08/02/99	11:09	242	41.2	33.6	13.00	4.90	22.1	78.8	47.3	21.6	331
21	08/03/99	10:57	242	30.7	34.8	10.90	4.80	20.4	66.2	41.6	20.4	318
22	07/28/99	13:49	232	53.1	33.7	17.00	5.25	24.0	86.5	56.0	23.2	392
23	08/02/99	13:01	198	54.9	34.6	17.20	5.30	23.3	88.1	57.5	23.2	395
24	07/28/99	14:34	187	57.4	34.0	18.60	5.50	23.7	91.2	60.0	24.4	392
25	07/28/99	13:11	138	49.1	33.3	15.30	5.05	22.4	85.0	52.6	22.2	374
26	07/28/99	11:04	118	32.4	32.5	11.40	4.50	19.1	60.9	43.2	19.1	319
27	07/29/99	17:17	78	56.0	32.6	17.40	4.80	21.0	81.9	56.3	20.0	368

1 kg/cm^2 = 0.09807 MPa.

Table 2. Experimental data taken at matched operating condition (2)

No.	P_c MPa (abs)	P_e MPa (abs)	P_c/P_e	T_c (°C)	T_e (°C)	$T_a - T_e$ (°C)	$\dot{m}_R$ (g/s)	Q_e (W)	COP	R_F (MPa kg^{-1}s)
1	1.511	0.688	2.20	55.5	27.7	9.0	6.28±0.70	897±12	3.54±0.48	131±15
2	1.354	0.619	2.19	51.1	25.1	11.4	5.62±0.64	827±89	3.41±0.37	131±16
3	1.570	0.688	2.28	57.0	27.4	7.2	6.19±0.68	913±125	3.30±0.46	142±16
4	1.188	0.610	1.95	45.9	22.0	5.0	5.61±0.65	866±84	3.71±0.37	103±13
5	1.629	0.649	2.51	58.6	25.6	9.2	5.85±0.66	824±101	3.07±0.38	168±20
6	1.688	0.688	2.45	60.1	27.7	9.1	6.21±0.69	860±12	2.99±0.42	161±19
7	1.384	0.610	2.27	51.9	23.0	9.9	5.56±0.64	815±83	3.34±0.35	139±17
8	1.345	0.605	2.22	50.7	22.1	10.0	5.50±0.63	831±82	3.41±0.34	134±16
9	1.256	0.619	2.03	48.1	23.6	10.5	5.71±0.66	856±85	3.63±0.37	112±14
10	1.198	0.575	2.08	46.2	21.5	9.6	5.30±0.62	807±70	3.52±0.31	117±15
11	1.256	0.629	2.00	48.0	24.3	9.9	5.75±0.65	892±94	3.61±0.39	109±13
12	1.972	0.747	2.64	66.8	30.6	4.8	6.71±0.73	883±152	2.99±0.52	183±21
13	1.178	0.580	2.03	45.5	21.6	10.4	5.30±0.61	835±73	3.64±0.33	113±14
14	1.217	0.590	2.06	46.8	21.5	11.1	5.38±0.62	898±77	3.79±0.33	116±14
15	1.296	0.561	2.31	49.2	20.7	12.3	5.09±0.60	766±65	3.22±0.28	145±18
16	1.864	0.668	2.79	64.3	26.6	8.0	5.98±0.67	787±108	2.88±0.40	200±23
17	1.893	0.757	2.50	65.0	30.6	4.9	6.86±0.75	926±156	3.06±0.52	166±19
18	1.247	0.585	2.13	47.7	21.9	11.7	5.35±0.62	816±73	3.48±0.32	124±15
19	2.040	0.629	3.24	68.3	25.1	11.0	5.56±0.63	695±88	2.52±0.32	254±30
20	1.374	0.580	2.37	51.6	21.6	12.0	5.26±0.61	779±72	3.31±0.31	151±19
21	1.168	0.570	2.05	45.2	20.4	14.4	5.24±0.62	814±67	3.52±0.30	114±14
22	1.766	0.615	2.87	62.0	23.2	10.5	5.50±0.63	747±83	2.81±0.32	209±25
23	1.786	0.619	2.89	62.5	23.2	11.4	5.56±0.64	738±83	2.80±0.32	210±25
24	1.923	0.639	3.01	65.7	24.4	9.6	5.74±0.65	739±89	2.85±0.35	224±27
25	1.599	0.595	2.69	57.8	22.2	11.1	5.36±0.62	751±75	2.92±0.30	187±23
26	1.217	0.541	2.25	46.8	19.1	13.4	4.94±0.60	753±57	3.34±0.26	137±18
27	1.805	0.570	3.17	62.9	20.0	12.6	5.07±0.60	678±64	2.78±0.27	243±31

$$Q_e = A_{eff} I + U_o A_c (T_a - T_e). \quad (8)$$

Eq. (8) can be expressed in the following relation:

$$\frac{Q_e}{I} = A_{eff} + U_o A_c \frac{T_a - T_e}{I} \quad (9)$$

Eq. (9) represents the thermal performance model of an ISAHP.

The experimental data for the test runs carried out for a fixed expansion valve opening (a mismatched condition) does not fit Eq. (9) very well, as shown in Fig. 6. This is due to liquid carryover to the compressor at under-load operation of evaporator, or superheating at evaporator at overload operation. Both will cause a variation of the absorbed energy Q_e. However, for the expansion valve opening adjusted manually during operation so as to keep the thermodynamic state at the suction port of the compressor close to saturated vapor state (within ± 2°C) and the exhaust temperature lower than 100°C, i.e. at *matched condition*, the experimental data (Tables 1 and 2) fit Eq. (9) fairly well, as shown in Fig. 7, with linear correlation coefficient $R = 0.969$. A_{eff} is found to be around 0.844 m^2 and $U_o A_c$ is 50.1 $W K^{-1}$ for the present prototype. The fitted value for the effective area A_{eff} would have a large uncertainty due to the data scattering at low Q_e/I as shown in Fig. 7. This implies that A_{eff} may not be a constant. Nevertheless, the performance of an ISAHP with $T_e < T_a$ and at matched condition is shown to follow Eq. (9).

From the determined values of A_{eff} and $U_o A_c$, the fraction of total rate of energy absorbed from ambient air, f_{air}, can be determined from the following relation derived from Eqs. (5) and (7):

$$f_{air} = Q_{air}/Q_e = (Q_e - A_{eff} I)/Q_e = 1 - aI \quad (10)$$

where $a = A_{eff}/Q_e$.

It is interesting to note that the experimental data for the ISAHP operating at $T_e < T_a$ and matched condition fit Eq. (10) very well, with linear correlation coefficient $R = 0.994$, as shown in Fig. 8. The coefficient a is found to be 0.000993 $m^2 W^{-1}$.

The correlation of Eq. (10) also reveals that the ISAHP absorbs more than 70 per cent energy from ambient air when $I < 300$ W m^{-2}. At clear weather with $I > 800$ W m^{-2}, the ISAHP absorbs less than 21 per cent energy from the ambient air.

The present experiment shows that Eqs. (9) and (10) can be used to characterize the performance of an ISAHP operating at $T_a > T_e$ and matched condition.

4.2. COP and Q_e of the ISAHP

The COP of the ISAHP ($= 1 + Q_e/W_{in}$) can be determined from the experimental data. Fig. 9 shows that COP of the ISAHP increases with increasing solar radiation I at low I. The rate of energy absorbed Q_e first increases with increasing solar radiation I for $I < 400$ W m^{-2} approximately and keeps approximately at a constant value

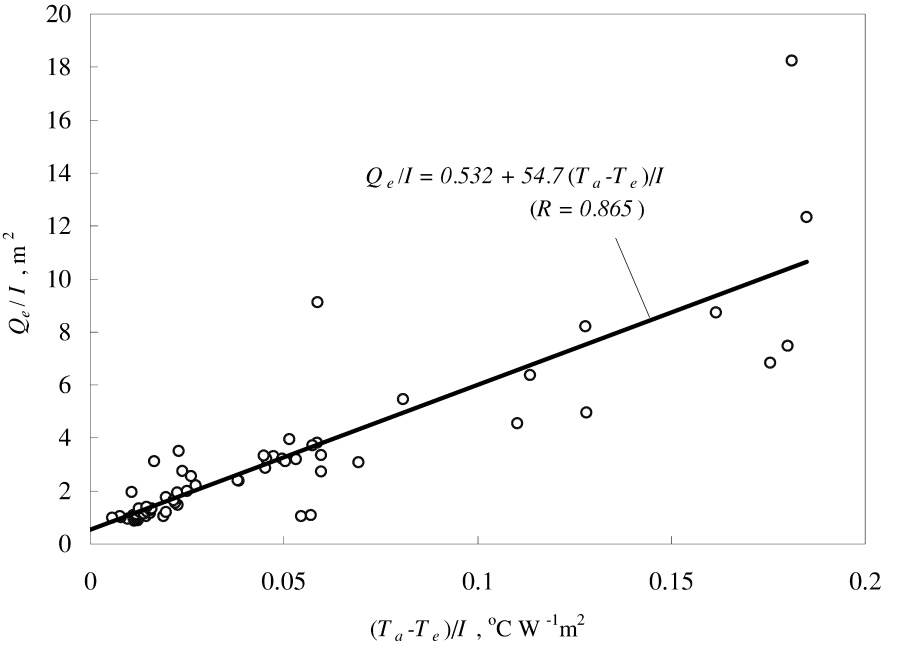

Fig. 6. Experimental data correlation for unscreened test data.

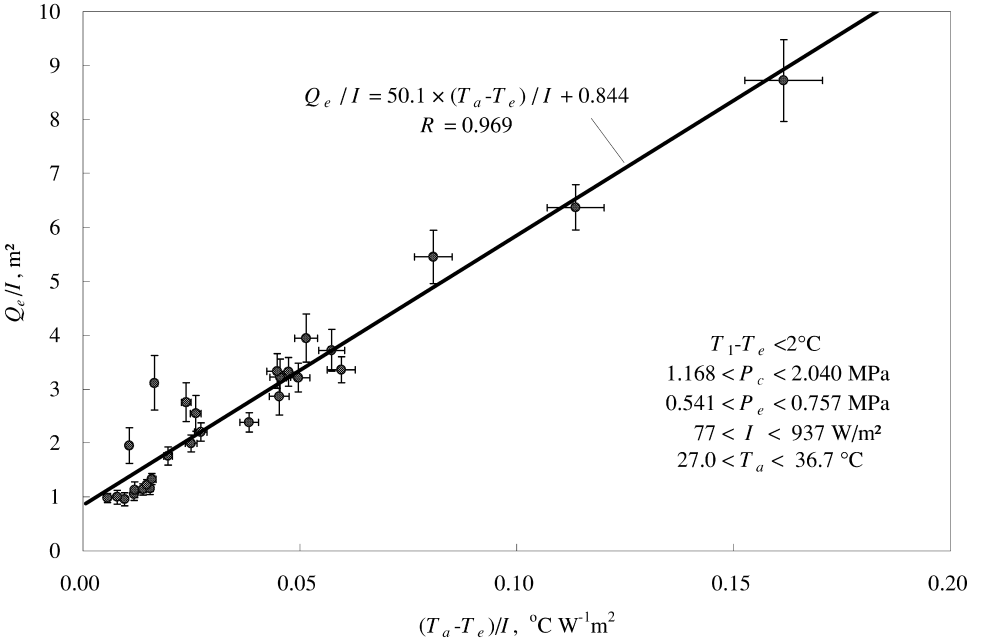

Fig. 7. Experimental data correlation for matched condition.

(about 850 W) for $I > 400$ W m^{-2}. At low solar radiation I, the total heat input to the collector/evaporator is small. This is an under-load operating condition that results in a low evaporating rate of R134a in the evaporator and the possibility of wet compression in the compressor. The expansion valve opening thus needs to reduce in order to protect the compressor from wet compression. The refrigerant mass flow rate decreases. This causes Q_e to decrease with decreasing I at low I.

At higher I, a wider expansion valve opening for increasing the refrigerant supply to the evaporator is necessary in order to achieve a matched operating condition. But the effect of valve opening is in turn limited by the compressor discharge capacity since the maximum cooling capacity for the compressor used in the present ISAHP is around 800 W. Hence, a higher I would not increase Q_e at all when I is higher than some value, around 400 W m^{-2} in the present experiment. This results in a roughly constant value of Q_e at $I > 400$ W m^{-2}.

The variation of Q_e with I described above seems to be in contradiction with the fact that the

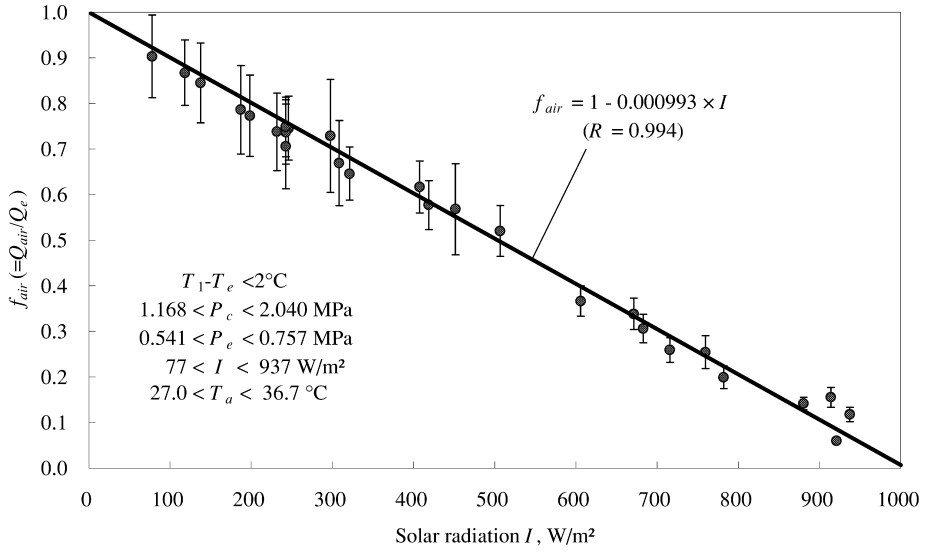

Fig. 8. Fraction of energy absorbed from ambient air f_{air} ($= Q_{air}/Q_e$).

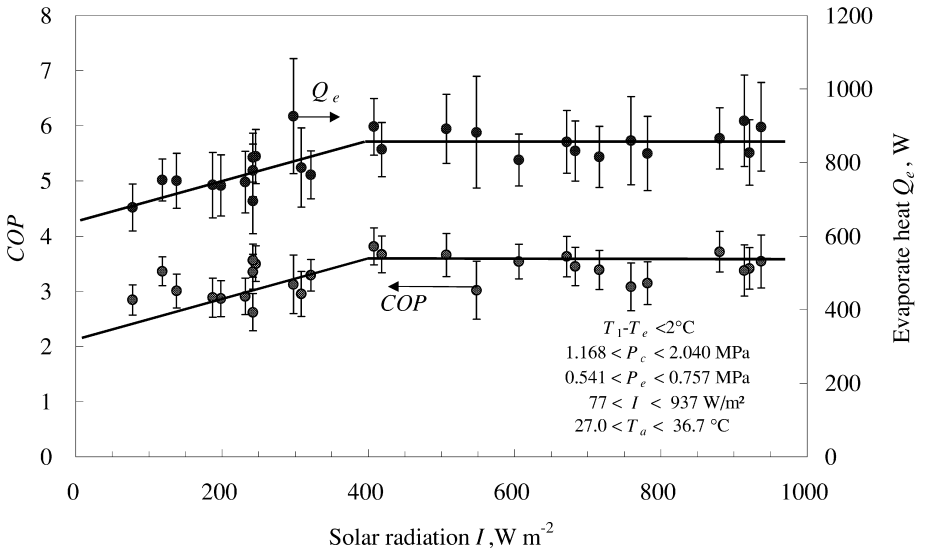

Fig. 9. Variation of COP and Q_e with I.

parameter a ($=A_{eff}/Q_e$) is constant as shown in Fig. 8 and Eq. (10). This may imply a constant Q_e for all the test results. However, a constant parameter a cannot actually assure a constant Q_e since the effective area A_{eff} may vary with I. The operation of ISAHP at low I usually takes place at a larger sun incident angle. This may cause A_{eff} to increase with increasing I, i.e. the same trend of Q_e variation with I.

On the other hand, Fig. 7 indicates that a value for A_{eff} can be obtained from experimental data fitting to Eq. (9). However, the data scattering at low Q_e/I will cause the fitted value of A_{eff} having a larger uncertainty. This may imply a possible variation of A_{eff}.

4.3. Variation of COP with water temperature

The measured COP of the ISAHP is found to decrease linearly with T_w as shown in Fig. 10. It is also noted from Fig. 11, that COP also decreases linearly with the temperature difference $T_w - T_e$ as found by Ito *et al.* (1999).

The measured COP in the present study ranges from 2.5 to 3.7 for $61°C > T_w > 25°C$ that is not as high as those obtained by other researcher (for example, Ito *et al.*, 1999). This is due to the lower volumetric efficiency of a small reciprocating-type compressor used in the experiment. A high COP will be obtained if a rotary or scroll compressor is used.

4.4. Variation of flow resistance of expansion valve

The adjustment of the expansion valve for obtaining a matched condition will lead to a change in flow resistance. From this, we can also understand how an ISAHP is operated at matched condition. The flow resistance of the expansion valve R_F is defined as

$$R_F = (P_c - P_e)/m_R. \tag{11}$$

R_F can be determined from the experimental data. Fig. 12 shows that R_F is linearly proportional to the pressure ratio indeed. The correlation is

$$R_F = 111.1(P_c/P_e - 1) \tag{12}$$

Combining Eqs. (11) and (12), we also obtain

$$m_R = P_e/111.1 \tag{13}$$

5. DISCUSSIONS AND CONCLUSION

In the present study, we studied the characteristics of an integral type solar-assisted heat pump water heater (ISAHP). The ISAHP consists of a Rankine refrigeration cycle and a thermosyphon loop that are integrated together to form a package heater. Both solar and ambient air energies are absorbed at the collector/evaporator and pumped to the storage tank via a Rankine refrigeration cycle and a thermosyphon heat exchanger. The condenser releases condensing heat of the refrigerant to the water side of the thermosyphon heat exchanger for producing a natural-circulation flow in the thermosyphon loop.

A 105-liter ISAHP using a bare collector and a small R134a reciprocating-type compressor was built and tested in the present study. The ISAHP was operated at $T_e < T_a$ and with a matched condition (near saturated vapor compression cycle

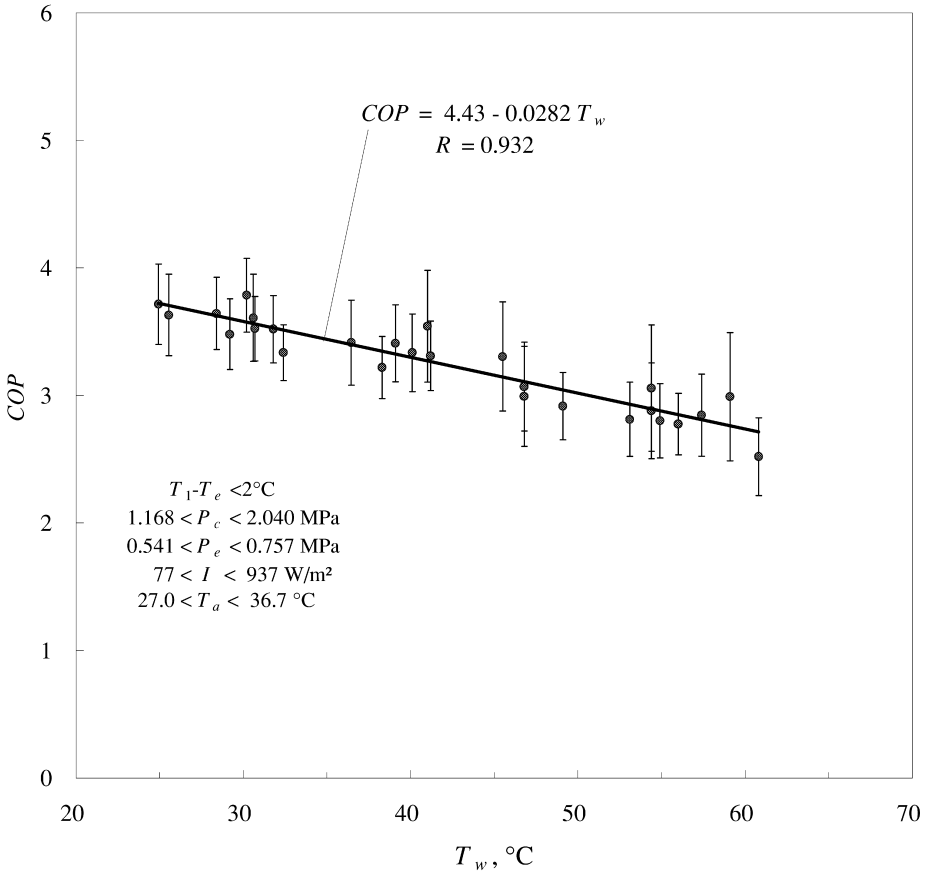

Fig. 10. Variation of COP with T_w.

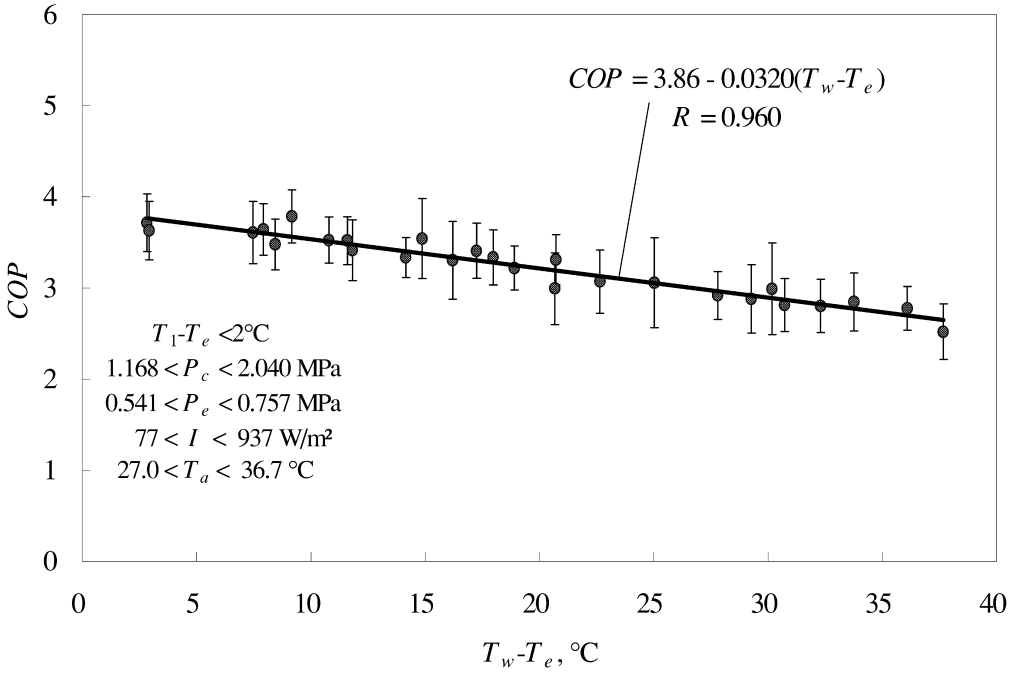

Fig. 11. Variation of COP with $T_w - T_e$.

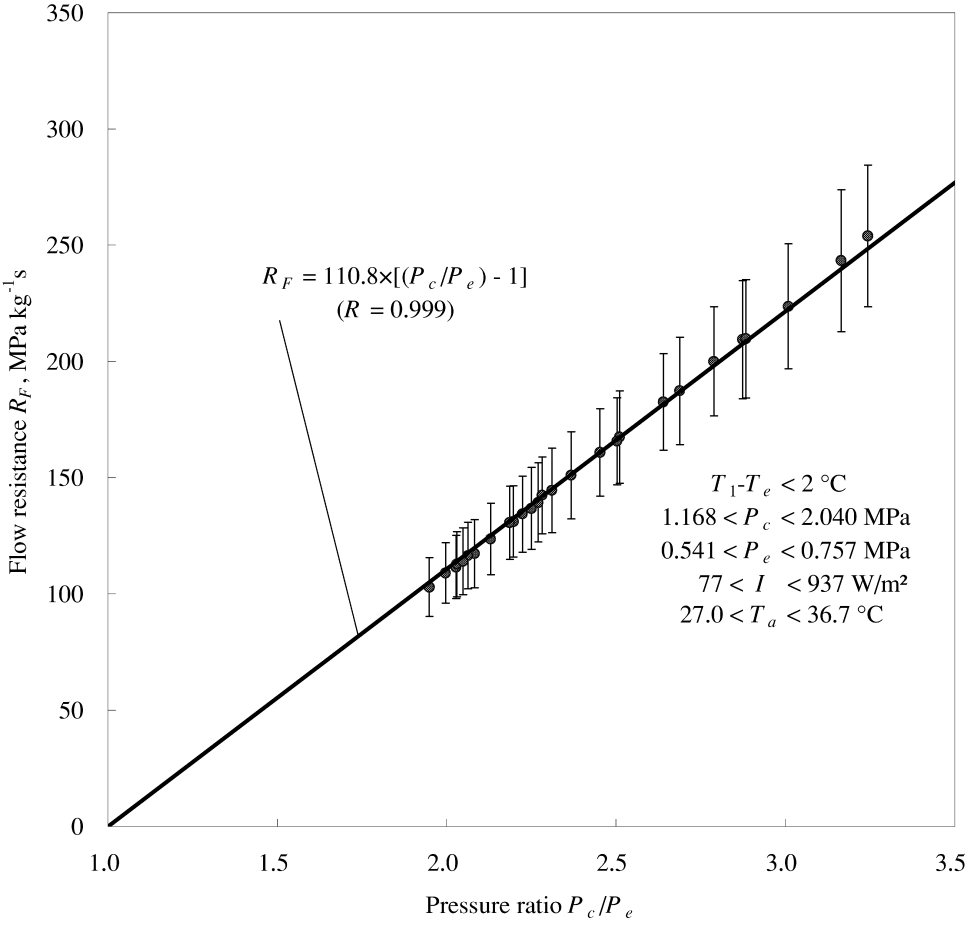

Fig. 12. Flow resistance of expansion valve.

and compressor exhaust temperature <100°C). A performance model, Eqs. (9) and (10), is derived and found to be able to fit the experimental data very well for the ISAHP operated at $T_e < T_a$ and a matched adjustment of the expansion valve. The test results show that the online adjustment of the expansion valve opening during operation will be helpful in keeping the compressor inlet temperature near a saturated-vapor state for obtaining a better performance of an ISAHP. This can be achieved by using an electronic expansion valve with a controller. The measured COP for the ISAHP built in the present study lies in the range 2.5–3.7 for $61°C > T_w > 25°C$. This is acceptable since the present ISAHP is operated at a matched condition that will assure the machine reliability. COP is also experimentally found to be linearly proportional to water temperature T_w, or the temperature difference $T_w - T_e$.

The present ISAHP is designed to operate at $T_e < T_a$ and thus is suitable for application in subtropical area like Taiwan whose ambient temperature is relatively high during winter seasons (>10°C). For the area that the ambient temperature is low in winter, the present ISAHP is still applicable if the collector sizing is changed and the refrigeration cycle is operated at lower pressure.

NOMENCLATURE

A_c	Total area of solar collector, m^2
A_{eff}	Effective area of solar collector, m^2
h_1	Enthalpy of refrigerant at suction of compressor, kJ kg^{-1}
h_4	Enthalpy of refrigerant at outlet of expansion valve, kJ kg^{-1}
I	Solar radiation intensity, W m^{-2}
m_R	Mass flow rate of refrigerant, kg s^{-1}
P_1	Compressor suction pressure, MPa
P_2	Compressor discharge pressure, MPa
P_c	Condensing pressure ($=P_2$), MPa
P_e	Evaporating pressure ($=P_1$), MPa
Q_e	Evaporating heat of refrigerant, W
Q_{air}	Heat from air, W
Q_{solar}	Heat from solar radiation, W
R	Linear correlation coefficient
R_F	Flow resistance of expansion valve, MPa kg^{-1} s

s	Entropy of refrigerant, kJ kg^{-1} K^{-1}
t	time, s
T_a	Ambient temperature,°C
T_c	Condensing temperature, °C
T_e	Evaporating temperature, °C ($=T_4$)
T_w	Water temperature in the tank, °C
T_1	Temperature at the entrance of compressor, °C
T_2	Temperature at the exit of compressor, °C
T_3	Temperature at the entrance of expansion valve, °C
T_4	Temperature at the exit of expansion valve, °C
U_0	Overall heat transfer coefficient from ambient air to solar collector surface, Wm^{-2} K^{-1}
v_1	Specific volume of refrigerant at suction of compressor, m^3 kg^{-1}
V_{SW}	Rate of sweep volume of piston, m^3 s^{-1}
α	Absorption coefficient of solar collector
η_v	Volumetric efficiency of compressor

Acknowledgements—The present study was supported by Energy Commission, Ministry of Economic Affairs, Taiwan.

REFERENCES

ASHRAE Handbook (1993) Fundamentals, American Society of Heating, Refrigerating and Air-Conditioning Engineers, Inc., 1993.

Huang B. J. and Chyng J. P. (1999) Integral type solar-assisted heat pump water heater. *Renewable Energy* **16**, 731–734.

Chaturvedi S. K., Chen D. T. and Kheireddine A. (1998) Thermal performance of a variable capacity direct expansion solar-assisted heat pump. *Energy Conversion Management* **39**, 181–191.

Chaturvedi S. K., Chiang Y. F. and Roberts A. S. (1980) Analysis of two-phase flow solar collectors with applications to heat pump. ASME Paper 80-WA/Sol-32.

Chaturvedi S. K. and Shen J. Y. (1984) Thermal performance of a direct expansion solar-assisted heat pump. *Solar Energy* **33**(2), 155–162.

Hino T. (1995) Performance evaluation of an ambient-energy heat pump system. *ASHRAE Transactions: Research* **101**, 386–393.

Ito S., Miura N. and Wang K. (1999) Performance of a heat pump using direct expansion solar collectors. *Solar Energy* **65**(3), 189–196.

Kline S. J. and McClintock F. A. (1953) Describing uncertainties in single-sample experiment. *Mech. Eng.* **75**(1), 3–8.

O'Dell M. P., Mitchell J. W. and Beckman W. A. (1984) Design method and performance of heat pump with refrigerant-filled solar collectors. *ASME J. Solar Energy Eng.* **106**, 159–164.

Sporn P. and Ambrose E. R. (1955) The heat pump and solar energy. *Proc. World Symp. Appl. Solar Energy, Phoenix, Arizona*, 1955